Dust storms from the Taklamakan Desert significantly darken snow surface on surrounding mountains

Yuxuan Xing[1], Yang Chen[1], Shirui Yan[1], Tenglong Shi[1], Xiaoyi Cao[1], Xiaoying Niu[1], Dongyou Wu[1], Jiecan Cui[1,2], Xin Wang[1,3], Wei Pu[1]

[1]Key Laboratory for Semi-Arid Climate Change of the Ministry of Education, College of Atmospheric Sciences, Lanzhou University, Lanzhou 730000, China

[2]Zhejiang Development & Planning Institute, Hangzhou 310030, China

[3]Institute of Surface-Earth System Science, Tianjin University, Tianjin 300072, China

Correspondence to: Wei Pu (puwei@lzu.edu.cn)

3 Method

3.2.4 Attribution of the spatial variation in snow albedo reduction

As noted above, the snow albedo reduction depends mainly on the dust content, snow optical effective radius (R_{eff}), snow depth (SD) and solar zenith angle (SZ). Snow optical effective radius and snow depth can be categorized as the snow properties (SP). Here we choose these three variables to discuss their fractional contributions to the spatial variability in snow albedo reduction. $\Delta\alpha$ can be expressed as

$$\Delta\alpha = f(\text{dust},\text{SP},\text{SZ}). \quad (10)$$

The spatial variability about snow albedo reduction due to dust can be described as

$$\Delta\alpha(\text{dust}) = f(\text{dust},\overline{\text{SP}},\overline{\text{SZ}}), \quad (11)$$

where $\overline{\text{SP}}$ and $\overline{\text{SZ}}$ indicate spatial-mean values of SP, and SZ. Similarly, we can obtain the following equations:

$$\Delta\alpha(\text{SP}) = f\left(\overline{\text{dust}},\text{SP},\overline{\text{SZ}}\right), \quad (12)$$

$$\Delta\alpha(\text{SZ}) = f\left(\overline{\text{dust}},\overline{\text{SP}},\text{SZ}\right). \quad (13)$$

We fit the $\Delta\alpha$ based on multiple linear regression, we can express it as

$$\Delta\alpha_{\text{fit}} = a\times\Delta\alpha(\text{dust}) + b\times\Delta\alpha(\text{SP}) + c\times\Delta\alpha(\text{SZ}), \quad (14)$$

where $\Delta\alpha_{\text{fit}}$ is the fitted snow albedo reduction, and a, b, c represent the regression coefficients. As a result, we can use $\Delta\alpha_{\text{fit}}$ to replace $\Delta\alpha$ to access the contribution to spatial variation of individual variables, Eq. (14) can be written as follows:

$$\Delta\alpha_{\text{fit}} - \overline{\Delta\alpha_{\text{fit}}} = a\times(\Delta\alpha(\text{dust}) - \overline{\Delta\alpha(\text{dust})}) + b\times(\Delta\alpha(\text{SP}) - \overline{\Delta\alpha(\text{SP})}) + c\times(\Delta\alpha(\text{SZ}) - \overline{\Delta\alpha(\text{SZ})}), \quad (15)$$

where we use $\Delta\alpha_{\text{fit}} - \overline{\Delta\alpha_{\text{fit}}}$ represent snow albedo reduction anomaly ($\Delta\alpha_{\text{fit}}^{\text{anomaly}}$). After, Eq. (15) can be written as

$$\Delta\alpha_{\text{fit}}^{\text{anomaly}} = \text{a}\times\Delta\alpha_{\text{anomaly}}(\text{dust}) + \text{b}\times\Delta\alpha_{\text{anomaly}}(\text{SP}) + \text{c}\times\Delta\alpha_{\text{anomaly}}(\text{SZ}). \quad (16)$$

According to Pu et al. (2019) and Cui (2021), the fractional contribution of dust to the spatial variability in snow albedo reduction (F_{dust}) can be written as

$$F_{\text{dust}}=\frac{1}{n}\sum_{i=1}^{n}\frac{(a\times\Delta\alpha_{\text{anomaly}}(\text{dust}))^2}{X_i}, \tag{17}$$

$$X_i=\left(a\times\Delta\alpha_{\text{anomaly}}(\text{dust})_i\right)^2+\left(b\times\Delta\alpha_{\text{anomaly}}(\text{SP})_i\right)^2+\left(c\times\Delta\alpha_{\text{anomaly}}(\text{SZ})_i\right)^2. \tag{18}$$

where n represent the length of the data set. Similarly, we can get the F_{SP} and F_{SZ}.

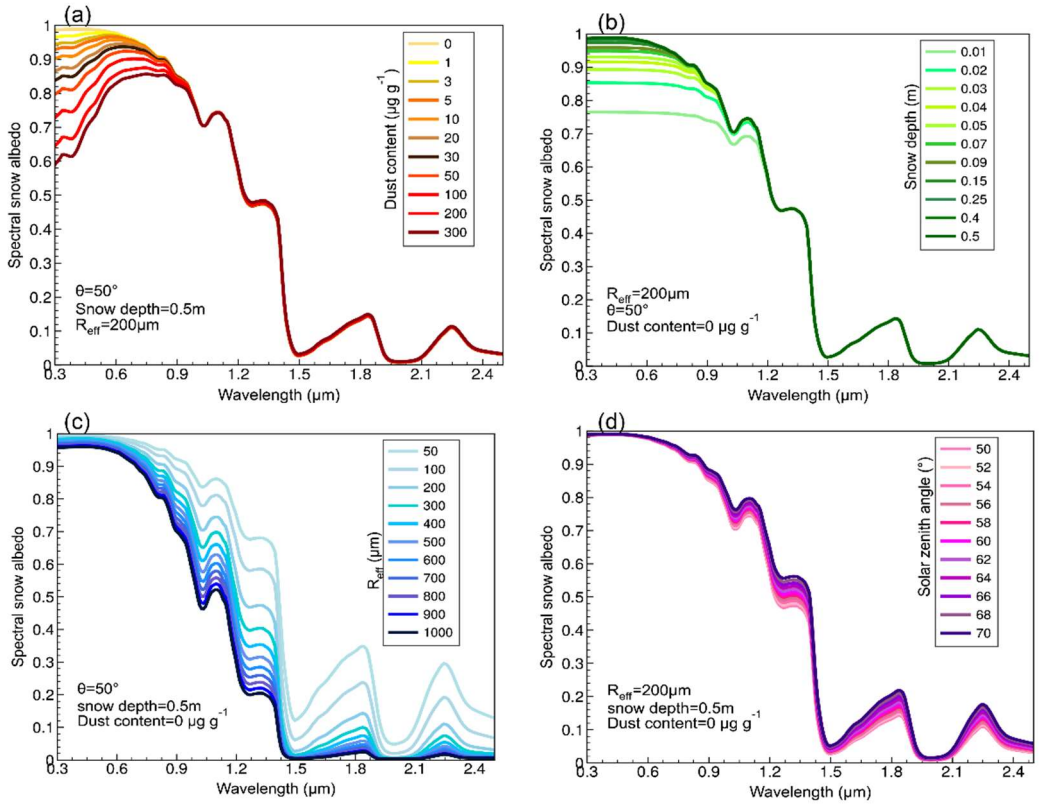

Figure S1. Variations in spectral snow albedo due to (a) dust content (μg g^{-1}), (b) snow depth (m), (c) snow grain size (μm), and (d) solar zenith angle (∘) while the other three parameters are kept constant.

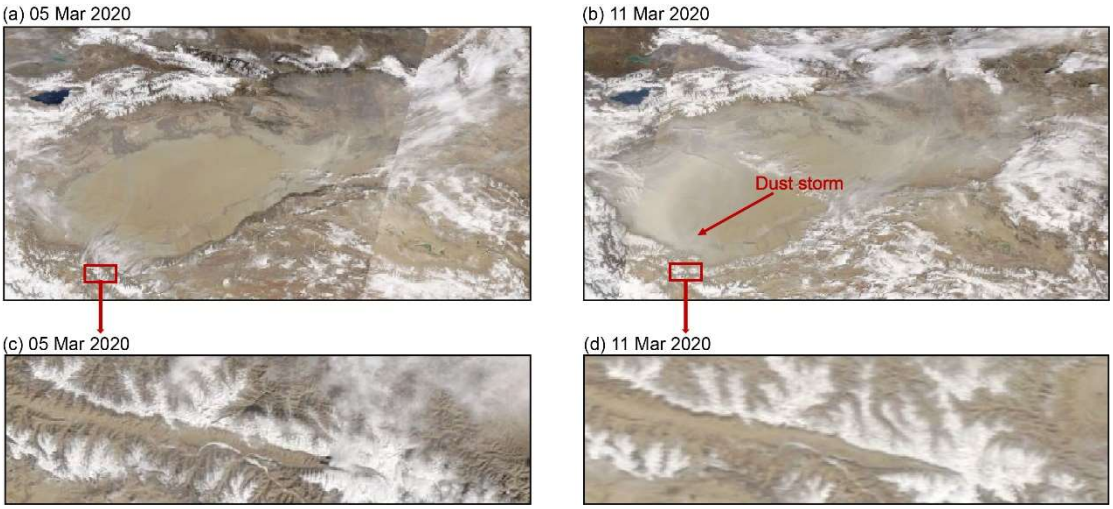

Figure S2. Satellite observations during the 05–11 March 2020 severe dust event across the Kunlun Mountains. (a, c) Terra/MODIS satellite true-color images acquired on 05 March 2020, prior to the dust storm. (b, d) Terra/MODIS satellite images acquired on 11 March 2020, with significant snow darkening across the Kunlun Mountains after the dust storm.

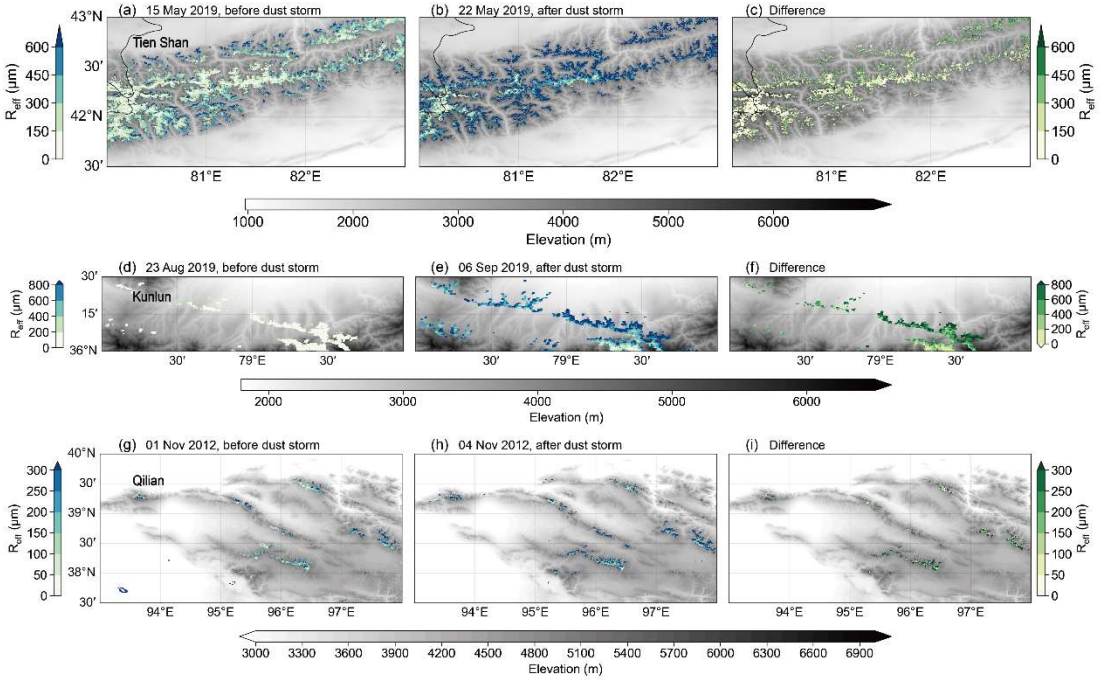

Figure S3. Spatial distributions of the average values and differences of R_{eff} across the (a-c) Tien Shan, (d-f) Kunlun Mountains and (g-i) Qilian Mountains, respectively.

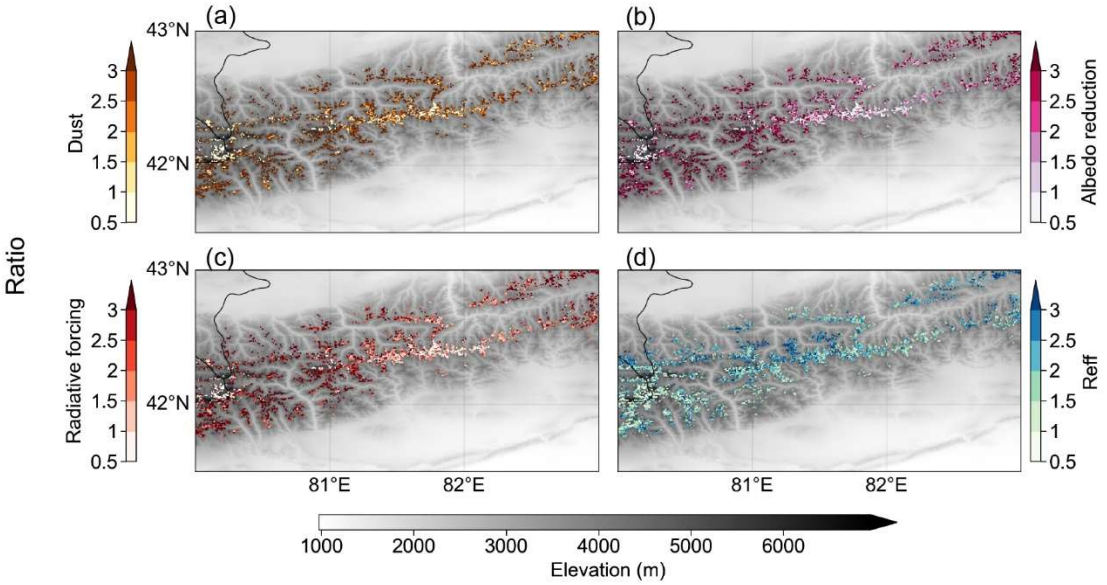

Figure S4. Spatial distribution of the ratios between 15 May 2019 and 22 May 2019 of (a) dust, (b) albedo reduction, (c) radiative forcing and (d) $R_{eff.}$ The background images in (a-d) show the elevation of Tien Shan.

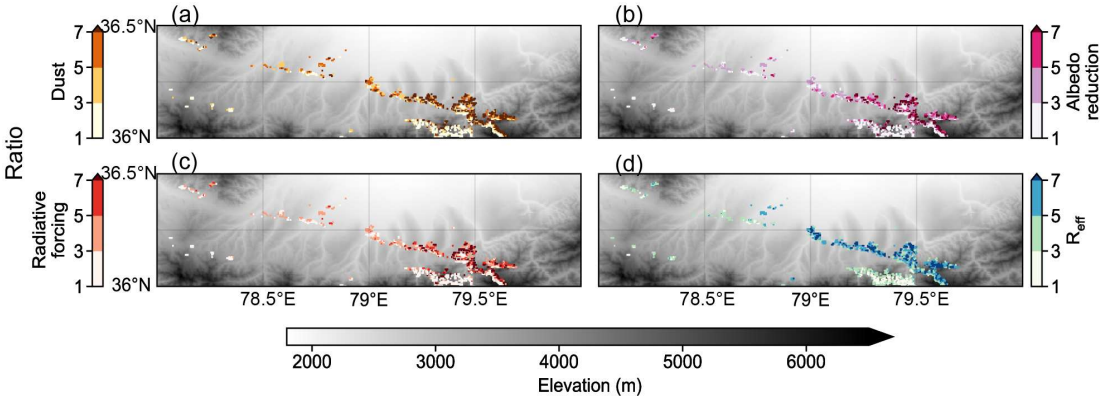

Figure S5. Spatial distribution of the ratio between 23 Aug 2019 and 06 Sep 2019 of (a) dust, (b) albedo reduction, (c) radiative forcing and (d) $R_{eff.}$ The background images in (a-d) show the elevation of Kunlun Mountains.

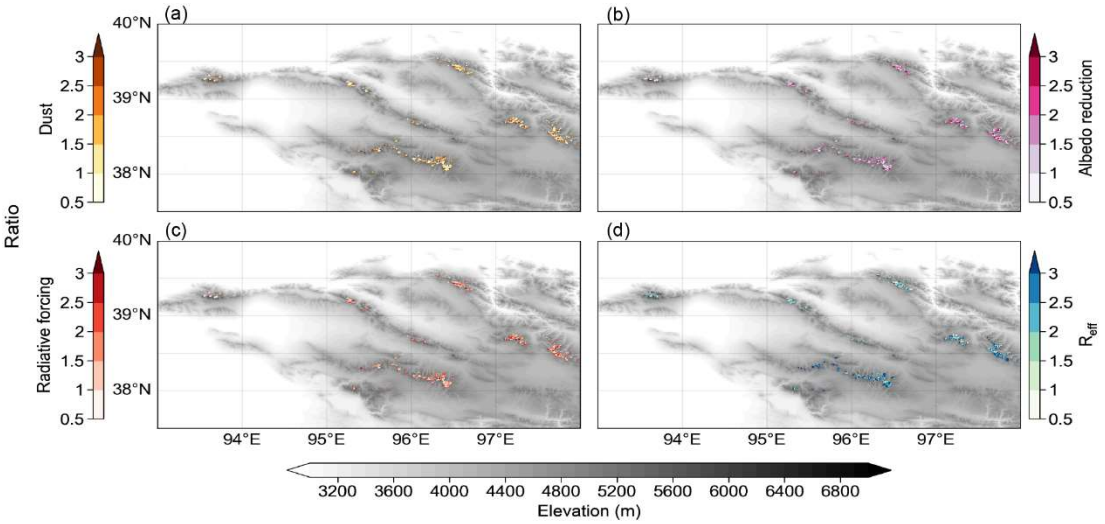

Figure S6. Spatial distribution of the ratio between 01 Nov 2012 and 04 Nov 2012 of (a) dust, (b) albedo reduction, (c) radiative forcing and (d) R_{eff}. The background images in (a-d) show the elevation of Qilian Mountains.

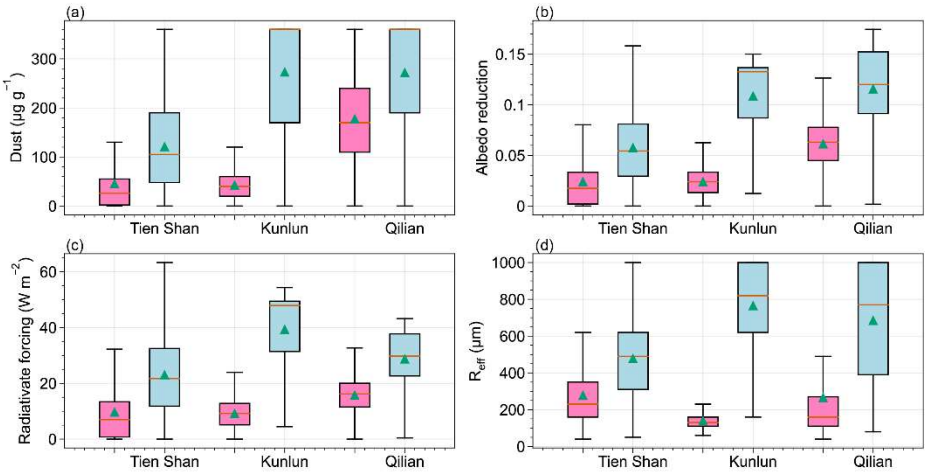

Figure S7. Statistics for regionally averaged (a) dust, (b) albedo reduction, (c) radiative forcing and (d) R_{eff} for Tien Shan, Kunlun Mountains and Qilian Mountains. The pink color shows 15 May, 2019, 23 August, 2019 and 01 November, 2012 before the dust storm in three regions. The blue color shows 22 May, 2019, 06 Sep, 2019 and 04 November, 2012 after the dust storm in three regions. The boxes denote the 25th and 75th quantiles, and the horizontal lines represent the 50th quantiles (medians); the averages are shown as blue triangle; the whiskers denote the 5th and 95th quantiles.

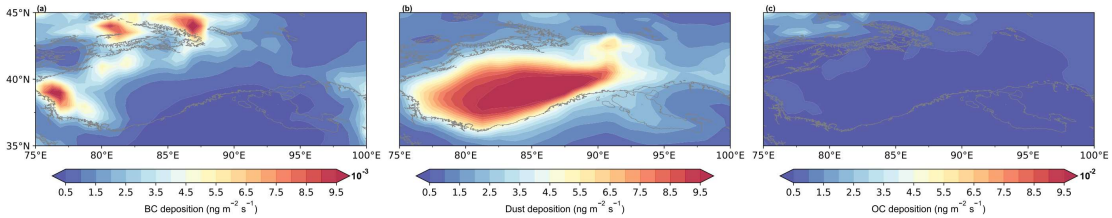

Figure S8. Spatial distributions of the averaged MERRA-2 (a) BC, (b) dust and (c) OC deposition rate from March to August 2019.